Gait & Posture 83 (2021) 280–286

Contents lists available at ScienceDirect

Gait & Posture

journal homepage: www.elsevier.com/locate/gaitpost

Full length article

The effect of hip muscle weakness and femoral bony deformities on gait performance

Ines Vandekerckhove [a,b,*], Mariska Wesseling [c,1], Hans Kainz [c,d,1], Kaat Desloovere [a,b], Ilse Jonkers [c]

[a] Department of Rehabilitation Sciences, KU Leuven, Leuven, Belgium
[b] Clinical Motion Analysis Laboratory, University Hospitals Leuven, Pellenberg, Belgium
[c] Department of Movement Sciences, KU Leuven, Leuven, Belgium
[d] Centre for Sport Science and University Sports, Department of Biomechanics, Kinesiology and Computer Science in Sport, University of Vienna, Vienna, Austria

ARTICLE INFO

Keywords:
Cerebral palsy
Hip muscle weakness
Femoral bony deformities
Gait performance

ABSTRACT

Background:Children with cerebral palsy (CP) present with a pathological gait pattern due to musculoskeletal impairments, such as muscle weakness and altered bony geometry. However, the effect of these impairments on gait performance is still unknown.

Research aim:This study aimed to explore the effect of hip muscle weakness and femoral deformities on the gait performance of CP and typical developing (TD) subjects.

Methods:6400 musculoskeletal models were created by weakening the hip extensors, abductors, adductors and flexors from 0% to 75 % and increasing the femoral anteversion angle (FAA) and neck shaft angle (NSA) from 20° to 60° and 120° to 160°, respectively. One TD and five CP gait patterns were imposed to each model and muscle forces were calculated. The effect of weakness and bony deformities on the capability gap (CG) at the hip, i.e. the lack in hip moment generating capacity to perform the gait pattern, was investigated using regression analysis.

Results:The CG of apparent equinus, stiff knee gait, TD gait, jump gait and true equinus increased with 0.080, 0.038, 0.015, 0.023 and 0.005 Nm/kg per 10 percent hip abductor weakness increase, with 0.211, 0.130, 0.056, 0.045 and 0.011 Nm/kg per 10 degrees FAA increase and with 0.163, 0.080, 0.036, 0.043 and 0.011 Nm/kg per 10 degrees NSA increase, respectively. Combined weakness and bony deformities explained 96 %, 85 %, 82 %, 65 %, 40 % and 35 % of the variance in the CG of apparent equinus, TD gait, stiff knee gait, jump gait, true equinus and crouch gait, respectively.

Significance:The results suggest that surgical correction of femoral deformities is more likely to be effective than strength training of hip muscles in enhancing CP gait performance. Jump gait, true equinus and especially crouch were more robust, while apparent equinus and stiff knee gait were limited by hip weakness and femoral deformities.

1. Introduction

Cerebral palsy (CP) is the most common motor disability in children [1] and is caused by a lesion in the developing brain, which results in permanent movement disorders, including gait [2]. To improve communication among clinicians, there have been several attempts at classifying gait deviations [3]. Apparent equinus, stiff knee gait, true equinus, crouch and jump gait are the most commonly reported gait patterns [3,4]. However, the use of these gait patterns in clinical practice necessitates the understanding of how underlying impairments contribute to these gait patterns [3].

Results of previous experimental studies investigating the relationships between impairments and gait deviations, were conflicting [5–7]. This is probably explained by the multifactorial nature of gait deviations with carry-over relations between impairments at one specific joint to motion of another joint [6]. To unravel this complex multicausality,

* Corresponding author at: KU Leuven, University of Leuven, Research Group for Neurorehabilitation (eNRGy), Weligerveld 1 blok 2 - box 7001, 3212, Pellenberg, Belgium.
E-mail address: ines.vandekerckhove@kuleuven.be (I. Vandekerckhove).
[1] Both authors contributed equally to this work

https://doi.org/10.1016/j.gaitpost.2020.10.022
Received 25 May 2020; Received in revised form 31 August 2020; Accepted 20 October 2020
Available online 25 October 2020

more research on identifying possible underlying impairments is needed.

Two impairments affecting gait in children with CP are muscle weakness and bony deformities. Especially, hip muscle weakness and femoral deformities have an important influence on gait as they affect the upright posture, trunk and pelvis stability and forward progression [2,8–10]. Both strength interventions and femoral osteotomies improve gait function [11,12]. However, it is still unclear which of both treatments has the most influence on improving gait.

Musculoskeletal simulation is a valuable tool to understand the complex relationship between underlying impairments and gait performance defined as the ability to achieve a walking pattern [13]. The capability gap (CG) is a simulation-based outcome measure that represents the discrepancy between the moments required to perform a motor task and the moments a participant can generate, and is therefore used to quantify gait performance [14,15]. If a CG appears, the neuromuscular adaptations, e.g. increased and reduced plantar flexor activity to compensate for its weakness and contracture, respectively [16], are not sufficient in maintaining a gait pattern. Afschrift et al. [14] found that typical developing (TD) gait could not be achieved anymore from 40 % of overall muscle weakness, where the CG became present. Additionally, TD gait was found to be unaffected by isolated weakness of hamstrings, psoas, but affected from 60 % and 80 % of weakness of gluteus medius and plantar flexors, respectively [17]. For crouch gait, less gluteus medius and plantar flexor strength was required [9]. Recently, Pitto et al. [15] developed a simulation platform that uses the CG as outcome measure to evaluate the effects of simulated surgeries to correct hip anteversion on CP gait performance. However, the influence of hip muscle weakness and femoral deformities on the CG of different gait patterns has never been investigated.

This study therefore aimed to investigate the effect of hip muscle weakness and femoral deformities (increased femoral anteversion angle (FAA) and neck shaft angle (NSA)) on the CG at the hip of the most commonly reported CP gait patterns. Hip muscle weakness (hypothesis 1.a) and femoral deformities (hypothesis 2.a) were expected to impair gait (as reflected in increased CG). Regarding the gait patterns, TD gait was expected to be affected to a larger extend by muscle weakness (hypothesis 1.b) and bony deformities (hypothesis 2.b) than CP gaits. As bony deformities affect the moment arms and muscle-lengthening properties of multiple muscles [18,19], bony deformities were expected to have a larger effect on the CG at the hip than isolated muscle weakness (hypothesis 3).

2. Methods

2.1. Experimental data

Five children with CP, who each walked with a different pathological gait pattern, and one TD child were analyzed retrospectively (Table 1). A more extended version of the Plug-in Gait marker set, including 35 surface markers, was placed on each participant [20]. Marker trajectories were collected at self-selected speed using a 12-camera three-dimensional motion capture system (Vicon, Oxford Metrics, UK) at a sampling rate of 100 Hz. Ground reaction forces were simultaneously measured with two force plates (Advanced Mechanical Technology Inc., Watertown, MA, sampling rate of 1000 Hz). Written informed consents were signed by the children's parents, in accordance with the ethical committee of University Hospital Leuven (Leuven/Pellenberg, Belgium).

2.2. Modeling and simulations

In SIMM (Motion Analysis Corp., Santa Rosa, CA) a generic model with 19 degrees of freedom (DOF) and 88 muscles was scaled to the anthropometry and weight of the TD child [21]. The model included six DOF at the pelvis, three rotational DOF at the hip joint and between the pelvis and torso, and one DOF at the knee and ankle joint. After the scaled model was created, bony deformities were induced in the model with the deform tool in SIMM [22]. In order to include a variety of femoral deformities ranging from pathological values of CP children to normal adult values [23], 25 models were created with FAA ranging from 20° to 60° and NSA ranging from 120° to 160° in steps of 10°, inducing altered muscle lengths and paths.

Model definition of the 25 SIMM models was modified for OpenSim in MATLAB (MatlabR2017a) [13] and the maximum isometric muscle force (MIMF) of the generic model was scaled to the subject's weight (Eq. 1) [24,25]. Due to the small body weight of the TD child, this scaling method resulted in unrealistic muscle activations even when using the model without muscle weakness and altered femoral geometry. Hence, we scaled the MIMF of the generic model using Eq. 2. This way, the simulations led to reasonable activations (did not attain maximal activations during a TD gait cycle). Furthermore, this did not influence the contribution of the reserve moment actuators (i.e. reserve moments activated if no feasible solution was found during static optimization).

$$F_{max}^{scaled} = \left(F_{max}^{generic} \times \left(\frac{M^{scaled}}{M^{generic}} \right)^{\frac{2}{3}} \right) \quad (1)$$

$$F_{max}^{scaled} = \left(F_{max}^{generic} \times \left(\frac{M^{scaled}}{M^{generic}} \right)^{\frac{2}{3}} \right) \times \frac{3}{2} \quad (2)$$

with F_{max}^{scaled} and $F_{max}^{generic}$ representing the MIMF of each muscle and M^{scaled} and $M^{generic}$ representing the body mass of the scaled models and the generic model, respectively.

From the 25 models with bony deformity, 6375 additional models were created in MATLAB by introducing different levels of muscle weakness for the hip extensor (gluteus maximus), abductors (gluteus medius and minimus), adductors (adductor longus, adductor brevis, adductor magnus and pectineus) and flexors (iliacus and psoas) muscle groups of both legs. The MIMF of the four muscle groups were decreased in steps of 25 % to simulate 25 %, 50 % and 75 % of muscle weakness. The initial 25 models represented the models without muscle weakness (0% of muscle weakness).

For the TD child, joint angles were calculated with the Kalman smoothing algorithm [26] and joint moments were calculated using the

Table 1
Participant information.

	TD01	CP01	CP02	CP03	CP04	CP05
Gait Pattern	TD gait	Apparent equinus	Stiff knee gait	True equinus	Crouch	Jump gait
Gender	Female	Male	Female	Female	Male	Male
GMFCS	/	II	II	I	II	II
Weight (kg)	30.4	18.7	21.9	20.7	17	25.1
Height (m)	1.39	1.17	1.23	1.17	1.11	1.28
Age (years)	9	6.5	7.9	7.5	8.7	6.3

Abbreviations in alphabetic order: GMFCS, Gross Motor Function Classification System; TD, typical developing.

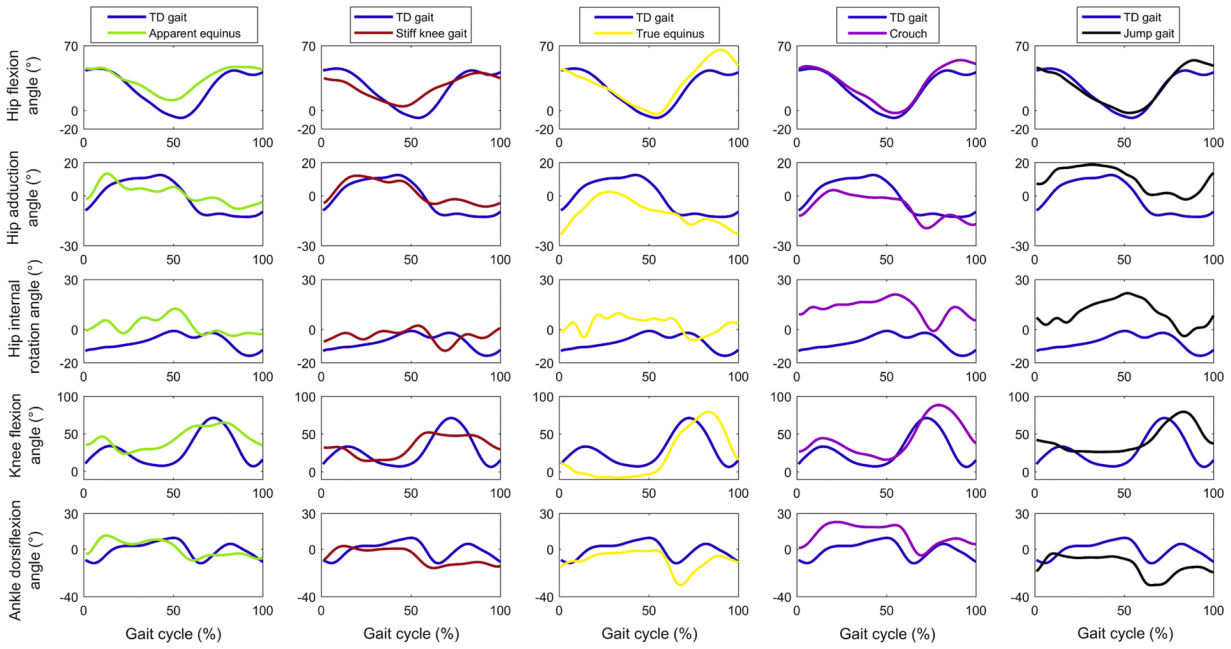

Fig. 1. Kinematics of TD gait, apparent equinus, stiff knee gait, true equinus, crouch and jump gait pattern calculated with a Kalman smoothing algorithm. Abbreviations in alphabetic order: TD, typical developing; °, degree; %, percentage.

inverse dynamic tool in OpenSim (Fig. 1 and Supplementary Fig. 1).

To apply the different gait patterns to the TD model, the experimental data of the enrolled CP participants were scaled to the included TD reference model, using a previously published approach [15]. First, the CP kinematics (obtained from the scaled CP model with the Kalman smoothing algorithm, Fig. 1) were imposed to the scaled TD model and corresponding 3D marker trajectories were extracted. The magnitudes of the ground reaction forces and moments were scaled based on the body mass and body mass times height, respectively. The point of application of the GRF, expressed in the foot reference frame, was scaled based on the scale factor of the foot segment. Thereafter, using the kinematics and ground reaction forces, the joint moments required for the TD reference model to perform the desired motion were computed (Supplementary Fig. 1). Afterwards, static optimization was used to calculate the individual muscle forces and activations while minimizing squared muscle activation for all walking patterns (1 TD and 5 CP patterns). Reserve moment actuators were added to each DOF in the model to ensure successful simulation even with the 'weak' and 'deformed' models [27].

The CG at the hip was defined as the difference between the hip moments required for a certain gait pattern and the total hip moments delivered by the muscles and was therefore represented by the reserve hip torque actuators [14]. We calculated the maximal absolute value of the CG over the gait cycle for the three DOFs at the hip to determine the largest deficit in moment generating capacity of the model to reproduce a specific gait pattern (Fig. 2).

2.3. Statistical analysis

Simple linear regression analyses were performed to determine the relation between the CG at the hip and (i) hip muscle weakness (hypothesis 1.a) and (ii) femoral deformities (hypothesis 2.a). The independent variables were hip extensor, abductor, adductor and flexor weakness, FAA and NSA. The dependent variables were the CG of the three DOFs at the hip. The regression equations with regression coefficients (β) were calculated for the six gait patterns. We selected the analysis with the largest regression coefficient from the three DOFs at the hip (flexion/extension, adduction/abduction, internal/external rotation) per independent variable for each gait pattern to be included in

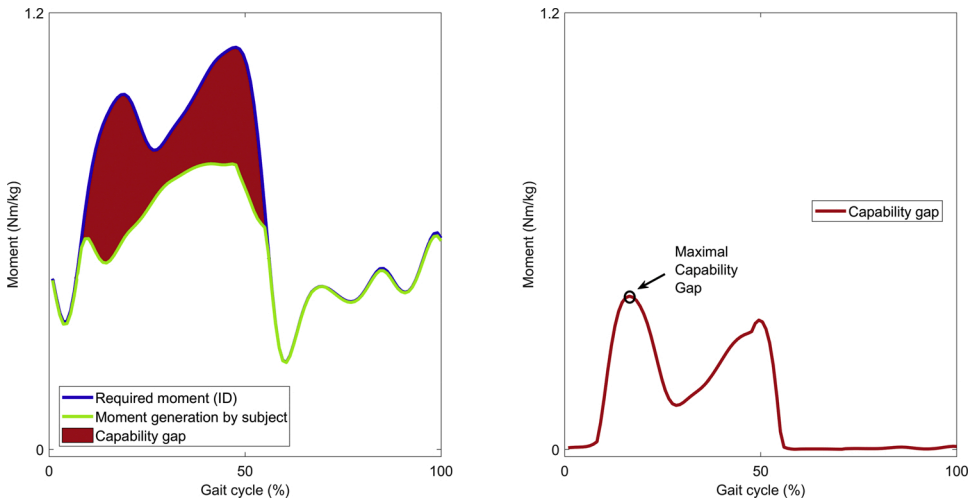

Fig. 2. (A) The difference between the required moment (inverse dynamics) to perform a specific gait pattern (blue line) and joint moment generated (static optimization) by the muscles (green line) of the model represents the lack in moment generating capacity, i.e. the capability gap (red area). In (B) the capability gap over the gait cycle is presented with the maximal absolute value encircled. (For interpretation of the references to colour in this figure legend, the reader is referred to the web version of this article).
Abbreviations in alphabetic order: Nm/kg, Newton-meters per kilogram body weight; %, percentage.

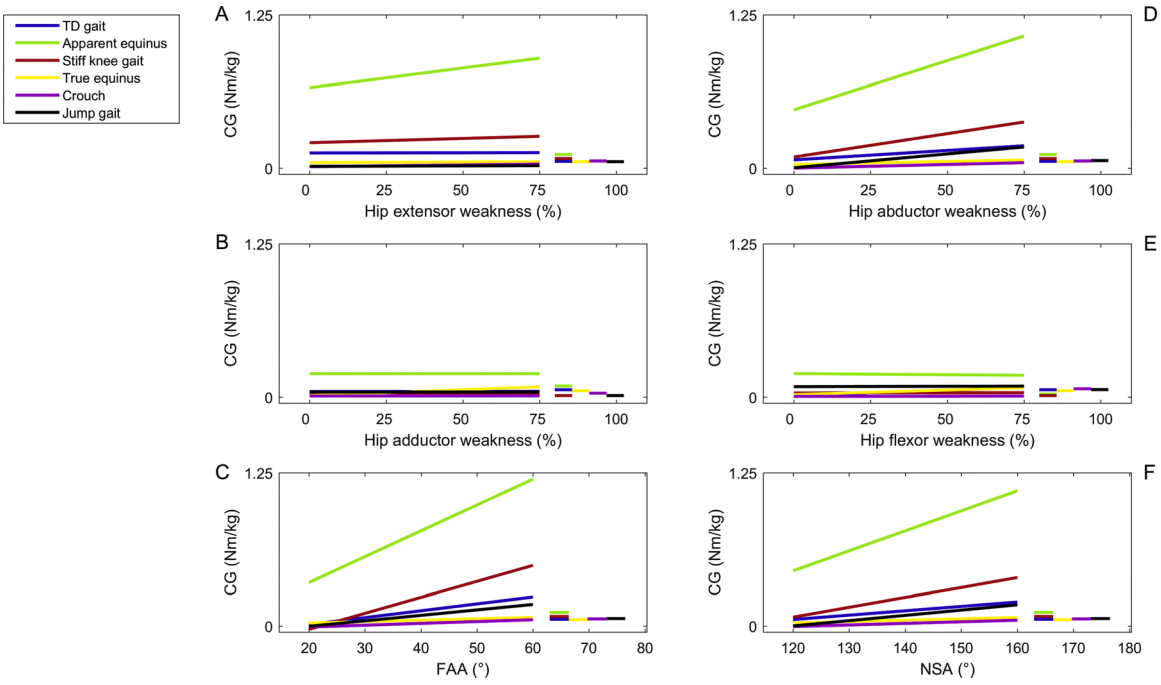

Fig. 3. Steepest regression lines with hip extensor weakness (A), hip adductor weakness (B), FAA (C), hip abductor weakness (D), hip flexor weakness (E) and NSA (F) as independent variables and the maximal absolute CG at the hip as dependent variable for the six different gait patterns (TD gait, apparent equinus, stiff knee gait, true equinus, crouch and jump gait). The horizontal lines on the right side of each graph represent 5% of the peak moments of the inverse dynamics. If the regression line surpasses the horizontal line, the independent variable has a relevant influence on the CG at the hip.
Abbreviations in alphabetic order: CG, capability gap; FAA, femoral anteversion angle; NSA, neck shaft angle; Nm/kg, Newton-meters per kilogram body weight; TD, typical developing; %, percentage.

further analyses. We judged if the effect of the independent variables on the CG were relevant based on the following criteria: (1) significant β, (2) $\beta > 0.001$ and (3) the maximal CG of the regression line exceeds 5% of the corresponding maximal required joint moments (ID) [17,25]. Analysis of covariance was used to determine if the regression coefficients of TD gait were significantly larger than regression coefficients of the CP patterns (hypothesis 1.b and 2.b).

Stepwise multiple regression analyses were performed to determine if bony deformities better predicted changes in the CG than muscle weakness (hypothesis 3). A bidirectional elimination procedure was used with a significance level of 0.05 and 0.10 as the criterion for the independent variables to be included or excluded, respectively. The root mean square error (RMSE), determination coefficients (R^2) and changes in determination coefficients (R^2 change) of the different regression equations for gait patterns were calculated. We reported the stepwise multiple regression analyses on the largest CG, regardless the DOF.

All analyses were performed in MATLAB. After applying the Bonferroni correction for multiple comparison considering the five hypotheses, the corrected α-level was 0.01 for all analyses.

3. Results

Across all relevant regression analyses, the dependent variable was attributed to the CG in hip adduction, flexion and internal rotation moment in 90 %, 5% and 5% of the analyses respectively.

3.1. Hip muscle weakness

The CG at the hip of the gait patterns increased when hip muscle weakness increased, except for crouch (Fig. 3 and Table 2). However, for apparent equinus, a CG decrease of -0.002 Nm/kg was found per 10 percent flexor weakness increase (Fig. 3.E and Table 2). Extensor weakness affected apparent equinus and stiff knee gait the most and significantly more than TD gait, with 0.032 and 0.007 Nm/kg CG increase per 10 percent weakness increase (Fig. 3.A and Table 2). Apparent equinus, stiff knee and jump gait experienced a larger effect of abductor weakness than TD gait per 10 percent increase in abductor weakness, with 0.080, 0.038, 0.023 and 0.015 Nm/kg CG increase, respectively, while true equinus experienced a smaller effect than TD gait with 0.005 Nm/kg CG increase (Fig. 3.D and Table 2). The CG of true equinus increased 0.009 Nm/kg per 10 percent adductor weakness increase, which was significantly larger than TD gait (Fig. 3.B and Table 2). A ten percent increase in flexor weakness increased the CG of TD gait and true equinus equally with 0.008 and 0.007 Nm/kg, respectively (Fig. 3.E and Table 2).

3.2. Femoral deformities

Increased bony deformities affected the CG at the hip of all gait patterns, except for crouch (Fig. 3 and Table 2). Furthermore, FAA had a larger effect on the CG than NSA. Ten degrees increase in FAA, increased the CG with 0.211, 0.130, 0.056, 0.045 and 0.011 Nm/kg for apparent equinus, stiff knee gait, TD gait, jump gait and true equinus, respectively, resulting in CG increases of the CP patterns being significantly different from TD gait (Fig. 3.C and Table 2). The CG of apparent equinus, stiff knee and jump gait, TD gait and true equinus increased with 0.163, 0.080, 0.043, 0.036 and 0.011 Nm/kg, respectively, when NSA increased with 10 degrees. This resulted in CG increases of the CP patterns that were significantly different from TD gait, except for jump gait (Fig. 3.F and Table 2).

3.3. Combined hip muscle weakness and femoral deformities

For the TD gait, FAA was the best predictor of the CG, followed by NSA, hip abductor and flexor weakness (Table 3). The regression equation with inclusion of these four independent variables explained 85 % of the variance in the CG. The best predictors for the CG of apparent equinus, stiff knee, crouch and jump gait were also FAA, NSA

Table 2
The largest regression coefficients of simple regression analyses for the maximal absolute CG at the hip of different gait patterns.

	Dependent variables					
	CG at the hip of different gait patterns					
Independent variables	TD gait	Apparent equinus	Stiff knee gait	True equinus	Crouch	Jump gait
Hip extensor weakness	**<0.001**	**0.032***,°	**0.007***,°	<0.001*	0.003*	<0.001*
Hip abductor weakness	**0.015***	**0.080***,°	**0.038***,°	**0.005***,°	0.006*,°	**0.023***,°
Hip adductor weakness	<0.001	**<0.001**	**<0.001**	**0.009***,°	<0.001*	**<0.001**
Hip flexor weakness	**0.008***	**−0.002***,°	**<0.001**°	**0.007***	<0.001*,°	**<0.001**°
FAA	**0.056***	**0.211***,°	**0.130***,°	**0.011***,°	0.015*,°	**0.045***,°
NSA	**0.036***	**0.163***,°	**0.080***,°	**0.011***,°	0.013*,°	**0.043***

The regression coefficients represent the increase or decrease in the CG (Nm/kg) per 10 percent and 10 degrees increase in hip muscle weakness and femoral deformities, respectively. Significant regression coefficients are indicated with an asterix and values in bold indicate that the maximal CG at the hip of the regression line is larger than 5% of the peak moments of the inverse dynamics. Regression coefficients with the symbol ° are significantly different from the regression coefficient of the CG at the hip of the TD gait pattern (analysis of covariance, Supplementary table 3). Abbreviations in alphabetic order: CG, capability gap; DOF, degrees of freedom; FAA, femoral anteversion angle; NSA, neck shaft angle; TD, typical developing.

Table 3
Results of stepwise multiple regression linear analyses for the maximal absolute CG at the hip of different gait patterns.

Dependent variables CG of different gait patterns	M	Independent variables						RMSE	R^2	R^2 change
TD gait	M1	FAA						2.52	0.48	0
	M2	FAA	NSA					2	0.67	0.19
	M3	FAA	NSA	HABD				1.51	0.81	0.14
	M4	**FAA**	**NSA**	**HABD**	**HF**			**1.37**	**0.85**	**0.03**
Apparent equinus	M1	FAA						10.57	0.42	0
	M2	FAA	NSA					7.9	0.68	0.25
	M3	FAA	NSA	HABD				4.01	0.92	0.24
	M4	**FAA**	**NSA**	**HABD**	**HE**			**2.95**	**0.96**	**0.04**
	M5	FAA	NSA	HABD	HE	HF		2.95	0.96	<0.01
Stiff knee gait	M1	FAA						5.89	0.47	0
	M2	FAA	NSA					4.77	0.66	0.18
	M3	FAA	NSA	HABD				3.5	0.82	0.16
	M4	**FAA**	**NSA**	**HABD**	**HE**			**3.45**	**0.82**	**0.01**
True equinus	M1	HADD						1.9	0.15	0
	M2	HADD	HF					1.79	0.25	0.1
	M3	HADD	HF	FAA				1.72	0.3	0.06
	M4	HADD	HF	FAA	NSA			1.65	0.36	0.05
	M5	**HADD**	**HF**	**FAA**	**NSA**	**HABD**		**1.6**	**0.4**	**0.04**
	M6	HADD	HF	FAA	NSA	HABD	HE	1.6	0.4	<0.01
Crouch	M1	FAA						1.59	0.14	0
	M2	FAA	NSA					1.49	0.24	0.11
	M3	FAA	NSA	HABD				1.41	0.33	0.09
	M4	**FAA**	**NSA**	**HABD**	**HE**			**1.39**	**0.35**	**0.02**
Jump gait	M1	FAA						3.62	0.22	0
	M2	FAA	NSA					3.11	0.42	0.2
	M3	**FAA**	**NSA**	**HABD**				**2.44**	**0.65**	**0.22**
	M4	FAA	NSA	HABD	HE			2.44	0.65	<0.01

As the CG was the largest in the hip frontal plane for all gait patterns, stepwise multiple regression analyses were performed on the CG in the hip frontal plane. The criterion for the independent variables to be included and excluded in the model was a significance level of 0.05 and 0.10, respectively. The models with the independent variables that best predicted the changes in the CG are in bold. Abbreviations in alphabetic order: CG, capability gap; FAA, femoral anteversion angle; HE, hip extensor weakness; HABD, hip abductor weakness; HADD, hip adductor weakness; HF, hip flexor weakness; M, model; M1, model 1; M2, model 2; M3, model 3; M4, model 4; M5, model 5; M6, model 6; NSA, neck shaft angle; R^2, determination coefficient; R^2 change, change in the determination coefficient with respect to previous model; RMSE, root mean square error; TD, typical developing.

and hip abductor weakness. Contrary to the TD gait, extensor weakness was the fourth best predictor of apparent equinus, stiff knee gait and crouch. These four variables explained 96 %, 82 % and 35 % of the variance in the CG of apparent equinus, stiff knee gait and crouch, respectively. 65 % of variance in the CG of jump gait was explained by FAA, NSA and abductor weakness. Adductor weakness was the best predictor of the CG for true equinus, followed by flexor weakness, FAA, NSA and abductor weakness. These five independent variables explained 40 % of the variance in the CG of true equinus.

4. Discussion

We explored the effect of hip muscle weakness and femoral deformities on the gait performance at the hip of different CP-specific walking patterns as quantified with the CG. In agreement with our hypothesis 1.a and 2.a, increasing muscle weakness and bony deformities impaired the gait performance. In contrast to hypothesis 1.b and 2.b, apparent equinus and stiff knee gait were more impaired than TD gait. Furthermore, femoral deformities had a larger influence on the CG at the hip than weakness for all analyzed gait patterns, except for true equinus and jump gait (hypothesis 3). Therefore, our hypotheses were only

partially confirmed.

Crouch gait appeared robust to weakness in all hip muscles, suggesting that hip muscle weakness is not a limiting factor to achieving crouch. Steele et al. [9] also reported that less abductor strength is required to perform crouch than TD gait. In contrast, of all muscle groups, strength in the abductors was found to be the most important for the performance of the other gait patterns (except for true equinus). This can be explained by the lack of other muscles to compensate for abductor weakness, while the availability of bi-articular muscles such as the hamstrings and rectus femoris [9,17], may compensate for extensor and flexor weakness, respectively. True equinus was the only pattern that was limited by adductor weakness, even more than abductor weakness, which may be explained by the observed increased hip abduction angles in the kinematics. Next to abductor weakness, flexor weakness limited the TD gait and true equinus performance, while extensor weakness affected the apparent equinus and stiff knee gait performance. Van der Krogt et al. [17] reported similar results for TD gait. In contrast to our hypothesis, apparent equinus and stiff knee gait required even more abductor and extensor strength than TD gait.

Femoral deformities, FAA more than NSA, affected the gait performance of all gait patterns, except crouch. Therefore, crouch appeared robust to femoral deformities, suggesting that femoral misalignment is not a limiting factor to maintain crouch gait. Although not fully, jump gait and true equinus appeared more robust to femoral deformities than TD gait. However, femoral deformities limited the performance of apparent equinus and stiff knee gait, even more than TD gait.

Increased FAA and NSA have a larger influence on the gait performance of apparent equinus, stiff knee and TD gait compared to weakness in just one hip muscle group, which may be explained by the bony deformities affecting the moment generating capacity of multiple muscles as decreases in moments arms of extensors, abductors, adductors, flexors and external rotators have been reported [18]. In contrast, jump gait and true equinus experienced an equal influence of abductor weakness and larger influence of adductor weakness than bony deformities, respectively. Increased hip internal rotation and abduction angle observed in the kinematics of jump gait and true equinus, respectively, may have compensated partially for the bony deformities [4,10].

As we expected, the performance of jump gait, true equinus and crouch were less impaired by combined hip weakness and femoral deformities than TD gait, suggesting that the neuromuscular adaptations were sufficient in maintaining these gait patterns. Especially the performance of crouch appeared to be robust.

In contrast, combined hip weakness and femoral deformities affected apparent equinus and stiff knee gait performance, more than and equal to TD gait performance, respectively. Apparent equinus and stiff knee gait may be more robust to other neuromuscular impairments. Contractures and spasticity of the iliopsoas and hamstrings and reduced voluntary control have been reported to contribute to apparent equinus [4,6,28]. Reduced muscle-tendon length, lengthening velocity and premature activity of the rectus femoris contribute to stiff knee gait [29,30].

We only examined the effect of hip muscle weakness and bony deformities on the CG. Therefore, caution is needed in the interpretation of the causality of the results. As other neuromuscular impairments, such as spasticity or contractures, may have less influence on apparent equinus and stiff knee gait performance, smaller increases in the CG may be expected if these impairments were additionally simulated. Furthermore, we did not model the impaired motor control nor did we tune the muscle optimal fiber length and tendon slack length to a CP model, which may have affected the magnitude of the CG [15].

To summarize, hip muscle weakness and femoral deformities affected TD and CP patterns. The CG was more sensitive to the bony deformities than hip muscle weakness, suggesting that surgical corrections of femoral geometry are more effective than strength training of hip muscles in restoring specific gait performance. From all analyzed walking patterns, the performance of apparent equinus and stiff knee gait were impaired by hip weakness and altered femoral geometry. In contrast, jump gait, true equinus and especially crouch were more robust to hip muscle weakness and bony deformities. Future studies should further unravel the complex multicausality of the gait patterns by exploring the effect of spasticity, contractures and altered motor control, as well as weakness and deformities around the other joints, on the CG.

Author contributions

All authors contributed either to the design, modeling and simulations, interpretation, writing, or editing. IV, HK, MW and IJ designed the experiment. Modeling and simulations were done by IV, HK and MW. Statistical tests were run by IV. Interpretation of the results was done by IV, HK, MW, KD and IJ. IV wrote the paper, which was edited by HZ, MW, KD and IJ. The entire process was supervised by IJ.

Declaration of Competing Interest

The authors declare that they have no conflict of interest.

Acknowledgements

This research was supported by IWT-TBM (Grant number: 140184). HK was funded by a H2020-MSCA individual fellowship (796120).

Appendix A. Supplementary data

Supplementary material related to this article can be found, in the online version, at doi:https://doi.org/10.1016/j.gaitpost.2020.10.022.

References

[1] K. Himmelmann, G. Hagberg, E. Beckung, B. Hagberg, P. Uvebrant, The changing panorama of cerebral palsy in Sweden. IX. Prevalence and origin in the birth-year period 1995-1998, Acta Paediatr. 94 (2005) 287–294, https://doi.org/10.1111/j.1651-2227.2010.01819.x.

[2] J. Gage, M. Schwartz, S. Koop, T. Novacheck, The Identification and Treatment of Gait Problems in Cerebral Palsy, 2nd ed., John Wiley Sons, 2009.

[3] E. Papageorgiou, A. Nieuwenhuys, I. Vandekerckhove, A. Van Campenhout, E. Ortibus, K. Desloovere, Systematic review on gait classifications in children with cerebral palsy: an update, Gait Posture 69 (2019) 209–223, https://doi.org/10.1016/j.gaitpost.2019.01.038.

[4] S. Armand, G. Decoulon, A. Bonnefoy-Mazure, Gait analysis in children with cerebral palsy, EFORT Open Rev. 1 (2016) 448–460, https://doi.org/10.1302/2058-5241.1.000052.

[5] A. Nieuwenhuys, E. Papageorgiou, S.-H. Schless, T. De Laet, G. Molenaers, K. Desloovere, Prevalence of joint gait patterns defined by a delphi consensus study is related to gross motor function, topographical classification, weakness, and spasticity, in children with cerebral palsy, Front. Hum. Neurosci. 11 (2017) 1–14, https://doi.org/10.3389/fnhum.2017.00185.

[6] E. Papageorgiou, C. Simon-martinez, G. Molenaers, E. Ortibus, A. Van Campenhout, K. Desloovere, Are spasticity, weakness, selectivity, and passive range of motion related to gait deviations in children with spastic cerebral palsy? A statistical parametric mapping study, PLoS One 14 (2019), e0223363, https://doi.org/10.1371/journal.pone.0223363.

[7] K. Desloovere, G. Molenaers, H. Feys, C. Huenaerts, B. Callewaert, P. Van de Walle, Do dynamic and static clinical measurements correlate with gait analysis parameters in children with cerebral palsy? Gait Posture 24 (2006) 302–313, https://doi.org/10.1016/j.gaitpost.2005.10.008.

[8] J. Zhou, E.E. Butler, J. Rose, Neurologic correlates of gait abnormalities in cerebral palsy: implications for treatment, Front. Hum. Neurosci. 11 (2017) 103, https://doi.org/10.3389/fnhum.2017.00103.

[9] K.M. Steele, M.M. van der Krogt, M.H. Schwartz, S.L. Delp, How much muscle strength is required to walk in a crouch gait? J. Biomech. 45 (2012) 2564–2569, https://doi.org/10.1016/j.jbiomech.2012.07.028.

[10] A. Carriero, A. Zavatsky, J. Stebbins, T. Theologis, S.J. Shefelbine, Correlation between lower limb bone morphology and gait characteristics in children with spastic diplegic cerebral palsy, J. Pediatr. Orthop. 29 (2009) 73–79, https://doi.org/10.1097/BPO.0b013e31819224d.

[11] M.N. Eek, R. Tranberg, R. Zügner, K. Alkema, E. Beckung, Muscle strength training to improve gait function in children with cerebral palsy, Dev. Med. Child Neurol. 50 (2008) 759–764, https://doi.org/10.1111/j.1469-8749.2008.03045.x.

[12] S. Ounpuu, P. DeLuca, R. Davis, M. Romness, Long-term effects of femoral derotation osteotomies: an evaluation using three-dimensional gait analysis, J. Pediatr. Orthop. 22 (2002) 139–145, https://doi.org/10.1097/00004694-200203000-00001.

[13] S.L. Delp, F.C. Anderson, A.S. Arnold, P. Loan, A. Habib, C.T. John, E. Guendelman, D.G. Thelen, OpenSim: Open source to create and analyze dynamic simulations of movement, IEEE Trans. Biomed. Eng. 54 (2007) 1940–1950, https://doi.org/10.1109/TBME.2007.901024.

[14] M. Afschrift, F. De Groote, J. De Schutter, I. Jonkers, The effect of muscle weakness on the capability gap during gross motor function: a simulation study supporting design criteria for exoskeletons of the lower limb, Biomed. Eng. Online 13 (2014) 111, https://doi.org/10.1186/1475-925X-13-111.

[15] L. Pitto, H. Kainz, A. Falisse, M. Wesseling, S. Van Rossom, H. Hoang, E. Papageorgiou, A. Hallemans, K. Desloovere, G. Molenaers, A. Van Campenhout, F. De Groote, I. Jonkers, SimCP: A simulation platform to predict gait performance following orthopedic intervention in children with cerebral palsy, Front. Neurorobot. 13 (2019) 54, https://doi.org/10.3389/fnbot.2019.00054.

[16] A.S. Fox, C.P. Carty, L. Modenese, L.A. Barber, G.A. Lichtwark, Simulating the effect of muscle weakness and contracture on neuromuscular control of normal gait in children, Gait Posture 61 (2018) 169–175, https://doi.org/10.1016/j.gaitpost.2018.01.010.

[17] M.M. van der Krogt, S.L. Delp, M.H. Schwartz, How robust is human gait to muscle weakness? Gait Posture 36 (2012) 113–119, https://doi.org/10.1016/j.gaitpost.2012.01.017.

[18] L. Scheys, A. Van Campenhout, A. Spaepen, P. Suetens, I. Jonkers, Personalized MR-based musculoskeletal models compared to rescaled generic models in the presence of increased femoral anteversion: effect on hip moment arm lengths, Gait Posture 28 (2008) 358–365, https://doi.org/10.1016/j.gaitpost.2008.05.002.

[19] L. Scheys, K. Desloovere, P. Suetens, I. Jonkers, Level of subject-specific detail in musculoskeletal models affects hip moment arm length calculation during gait in pediatric subjects with increased femoral anteversion, J. Biomech. 44 (2011) 1346–1353, https://doi.org/10.1016/j.jbiomech.2011.01.001.

[20] M. van der Krogt, M. Goudriaan, M. Petrarca, A. Balemans, M. Piening, G. Vasco, E. Castelli, K. Desloovere, J. Harlaar, A European consensus protocol for clinical gait analysis, Gait Posture 151 (2015) 10–17, https://doi.org/10.1145/3132847.3132886.

[21] H. Kainz, H.X. Hoang, C. Stockton, R.R. Boyd, D.G. Lloyd, C.P. Carty, Accuracy and reliability of marker-based approaches to scale the pelvis, thigh, and shank segments in musculoskeletal models, J. Appl. Biomech. 33 (2017) 354–360, https://doi.org/10.1123/jab.2016-0282.

[22] H. Kainz, B.A. Killen, M. Wesseling, F. Perez-Boerema, L. Pitto, J.M.G. Aznar, S. Shefelbine, I. Jonkers, A multi-scale modelling framework combining musculoskeletal rigid-body simulations with adaptive finite element analyses, to evaluate the impact of femoral geometry on hip joint contact forces and femoral bone growth, PLoS One 15 (2020) 1–18, https://doi.org/10.1371/journal.pone.0235966.

[23] M.F. Abel, D.R. Wenger, S.J. Mubarak, D.H. Sutherland, Quantitative analysis of hip dysplasia in cerebral palsy a study of radiographs and 3D reformatted images, J. Pediatr. Orthop. 14 (1994) 283–289.

[24] M.M. van der Krogt, L. Bar-On, T. Kindt, K. Desloovere, J. Harlaar, Neuro-musculoskeletal simulation of instrumented contracture and spasticity assessment in children with cerebral palsy, J. Neuroeng. Rehabil. 13 (2016) 64, https://doi.org/10.1186/s12984-016-0170-5.

[25] H. Kainz, M. Goudriaan, A. Falisse, C. Huenaerts, K. Desloovere, F. De Groote, I. Jonkers, The influence of maximum isometric muscle force scaling on estimated muscle forces from musculoskeletal models of children with cerebral palsy, Gait Posture 65 (2018) 213–220, https://doi.org/10.1016/j.gaitpost.2018.07.172.

[26] F. De Groote, T. De Laet, I. Jonkers, J. De Schutter, Kalman smoothing improves the estimation of joint kinematics and kinetics in marker-based human gait analysis, J. Biomech. 41 (2008) 3390–3398, https://doi.org/10.1016/j.jbiomech.2008.09.035.

[27] F.C. Anderson, M.G. Pandy, Static and dynamic optimization solutions for gait are practically equivalent, J. Biomech. 34 (2001) 153–161, https://doi.org/10.1016/S0021-9290(00)00155-X.

[28] M. Goldstein, D.C. Harper, Management of cerebral palsy: equinus gait, Dev. Med. Child Neurol. 43 (2001) 563–569, https://doi.org/10.1111/j.1469-8749.1982.tb13593.x.

[29] I. Jonkers, C. Stewart, K. Desloovere, G. Molenaers, A. Spaepen, Musculo-tendon length and lengthening velocity of rectus femoris in stiff knee gait, Gait Posture 23 (2006) 222–229, https://doi.org/10.1016/j.gaitpost.2005.02.005.

[30] J.A. Reinbolt, M.D. Fox, A.S. Arnold, S. Õunpuu, S.L. Delp, Importance of preswing rectus femoris activity in stiff-knee gait, J. Biomech. 41 (2008) 2362–2369, https://doi.org/10.1016/j.jbiomech.2008.05.030.